



DEPARTMENT OF
ELECTRICAL &
COMPUTER ENGINEERING



Improving Image Quality for Recognition

Rama Chellappa
Dept. of ECE and UMIACS
University of Maryland



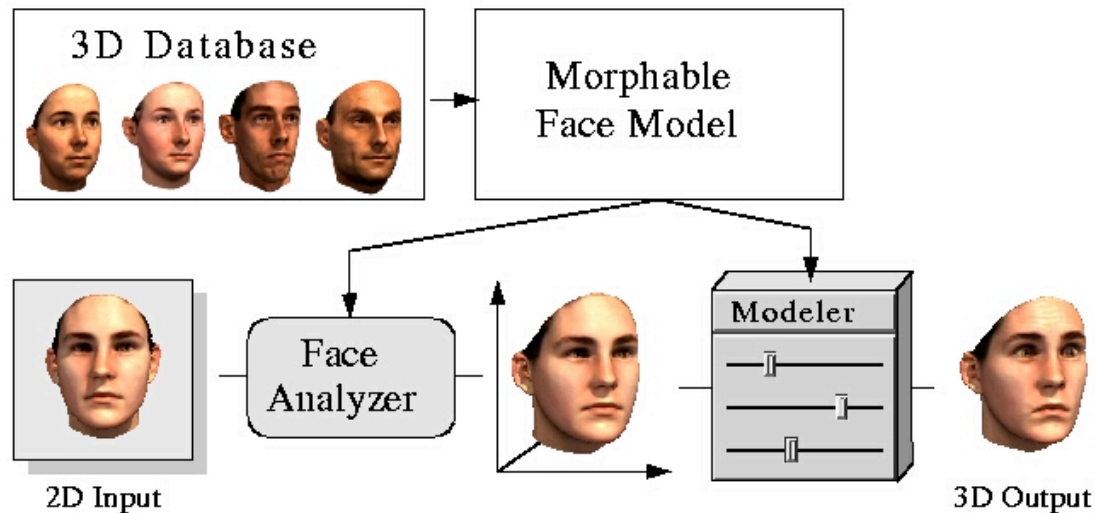
Things that Make Faces Look Bad

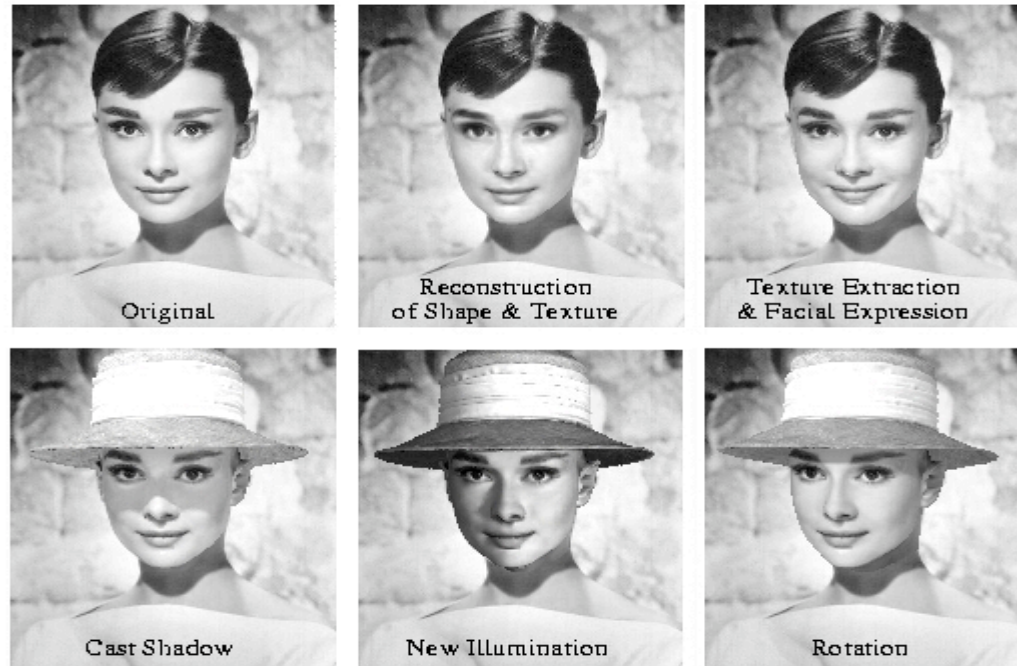
- Illumination
- Pose
- Motion
- Atmospherics
- Expressions
- Aging
- Disguises
- Effectiveness of improving the quality measured by the increase in recognition performance.
- For an academician, poor images offer more opportunities!

Morphable Models

- Similar to AAM and vectorized representation
- After manual initialization, align a novel 2D image to a morphable 3D model learnt from a set of training samples

Blanz and Vetter PAMI 2003





Recovered 3D shape and synthesized images

Computational cost, semi-
automatic.



FR 2002
VT 2002

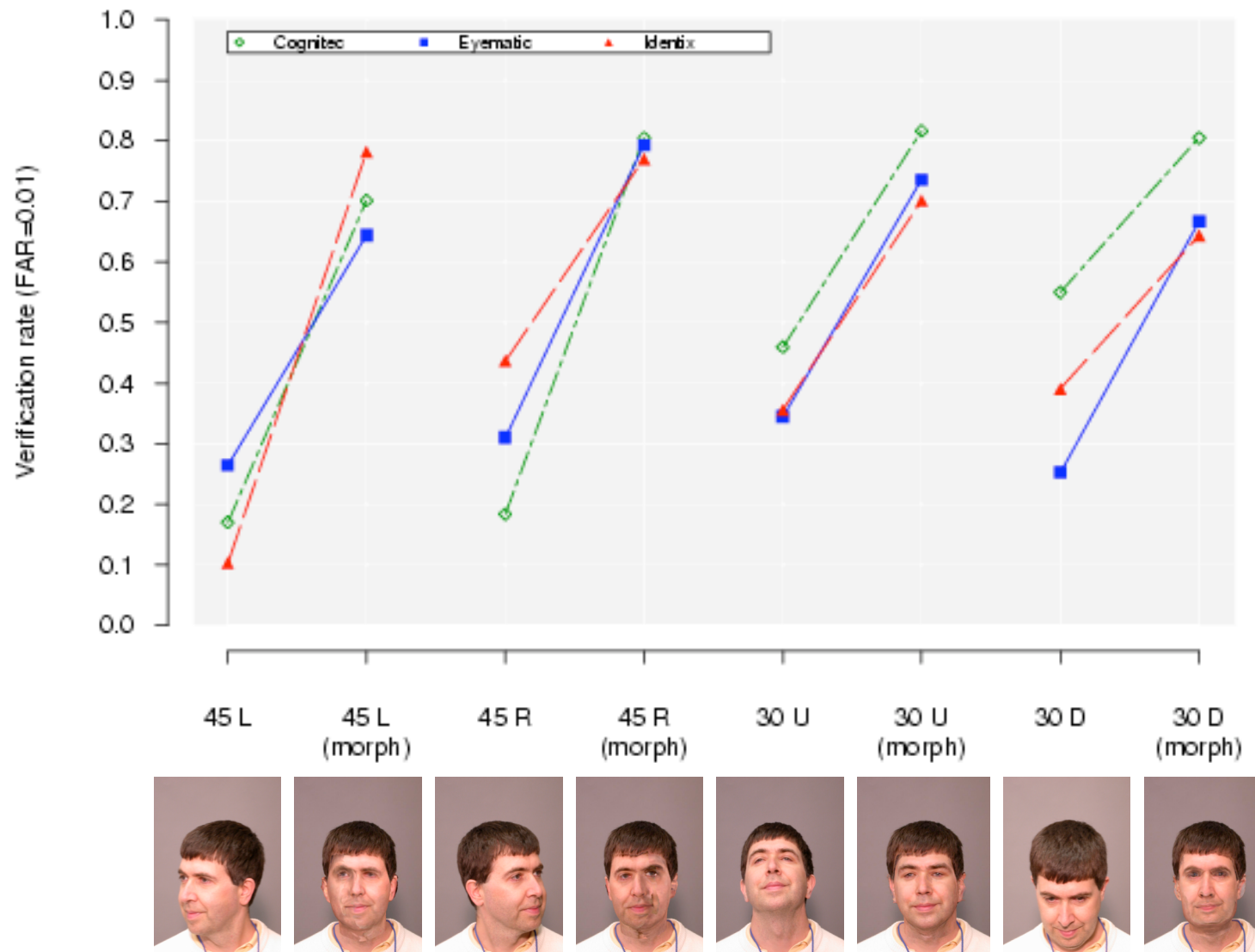
Medium Computational Intensity Test

3D Morphable Models





Pose & Morphable Experiment





Shape from Shading/ Photometric Stereo

- Use shape from shading algorithms for synthesizing frontal, illumination-normalized images. [Zhao and Chellappa, IJCV 2001]
- Images of an object generated by a moving light source can be spanned using a subspace of dimension 3. [Sashua, IJCV, 1997].
 - Add an ambient component – subspace becomes 4-D. [Yuille, et al, IJCV, 1999]
- With attached shadows – infinite dimensional [Belhumeur and Kriegman, IJCV, 1998]
 - Low-dimensional approximation [Basri and Jacobs, CVPR, 2001, PAMI, 2003]
 - Ramamurthi and Hanrahan [JOSA, 2001]
- Object specific samples [Except Sashua and Raviv, PAMI 2001]



Generalized Photometric Stereo

- Handles all appearances of all objects in a class
 - Human face class
- Rank constraint on the product of albedo and surface normal
 - Factorization of class-specific ensemble into two matrices
 - Albedo and surface normal
 - Blending linear coefficients and lighting conditions
- Class-specific ensemble
 - Exemplar images of different objects, each under different illumination. Goes beyond bilinear analysis (Freeman and Tenenbaum, CVPR 1997)
- To enable full recovery of albedo and surface normal
 - Integrability and symmetry constraints.
 - Zhou, Agarwal, Chellappa and Jacobs, IEEE Trans. PAMI feb. 2007.

- Pixel:

$$h = \rho \cos(\theta) = \rho \mathbf{n}^T \mathbf{s} = \mathbf{t}^T \mathbf{s}$$

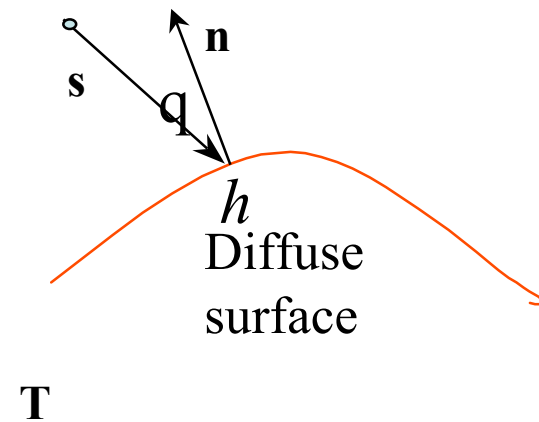
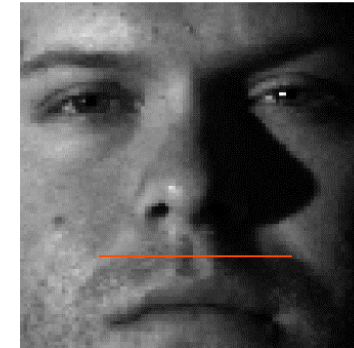
$$\mathbf{n} = [\hat{a}, \hat{b}, \hat{c}]^T, \quad \mathbf{t} = [a = \rho \hat{a}, b = \rho \hat{b}, c = \rho \hat{c}]^T$$

$$\rho = \sqrt{\mathbf{t}^T \mathbf{t}} = \sqrt{a^2 + b^2 + c^2}$$

- Image:

$$\begin{aligned} \mathbf{h}_{d \times 1} &= [h_1, h_2, \dots, h_d]^T \\ &= [\rho_1 \mathbf{n}_1^T \mathbf{s}_1, \rho_2 \mathbf{n}_2^T \mathbf{s}_2, \dots, \rho_d \mathbf{n}_d^T \mathbf{s}_d]^T \\ &= \mathbf{T}_{d \times 3} \mathbf{s}_{3 \times 1} \end{aligned}$$

- \mathbf{T} : shape matrix for one person
[Shashua IJCV'97]





Essentials of GPS



- Key derivations:

$$\begin{aligned}\mathbf{h}_{d \times n} &= \mathbf{T}\mathbf{s} = [\mathbf{T}_1, \mathbf{T}_2, \dots, \mathbf{T}_m] (\mathbf{f} \otimes \mathbf{I}_3) \mathbf{s} \\ &= \mathbf{W}_{d \times 3m} (\mathbf{f}_{m \times 1} \otimes \mathbf{s}_{3 \times 1})\end{aligned}$$

- Key properties:

- $\mathbf{W} = [\mathbf{T}_1, \mathbf{T}_2, \dots, \mathbf{T}_m]$ class-specific albedo-shape matrix for all faces.
- \mathbf{f} : illumination-invariant. Good for recognition.
- Bilinear in \mathbf{f} and \mathbf{s} .
- Learn \mathbf{W} from the training set.



Eigenface on PIE



Gallery	f_{08}	f_{09}	f_{11}	f_{12}	f_{13}	f_{14}	f_{15}	f_{16}	f_{17}	f_{20}	f_{21}	f_{22}	Average
Probe													
f_{08}	-	100	90	66	21	9	1	9	4	60	60	1	38
f_{09}	100	-	72	94	59	31	10	24	13	51	84	13	50
f_{11}	97	91	-	100	29	24	13	15	10	100	94	19	54
f_{12}	93	97	100	-	93	90	56	59	35	96	100	69	81
f_{13}	19	62	22	68	-	97	82	100	68	13	84	81	63
f_{14}	9	15	12	62	100	-	100	84	82	12	72	100	59
f_{15}	0	3	1	4	76	100	-	74	76	1	18	100	41
f_{16}	6	25	3	31	82	65	71	-	100	3	41	57	44
f_{17}	4	12	3	31	51	56	81	100	-	3	28	59	39
f_{20}	88	76	100	99	28	28	15	12	16	-	99	19	53
f_{21}	84	97	97	100	96	88	57	74	46	96	-	71	82
f_{22}	3	4	3	13	72	100	100	50	57	3	24	-	39
Average	46	53	46	61	64	62	53	54	46	40	64	54	54



Fisherface on PIE



Gallery	f_{08}	f_{09}	f_{11}	f_{12}	f_{13}	f_{14}	f_{15}	f_{16}	f_{17}	f_{20}	f_{21}	f_{22}	Average
Probe													
f_{08}	-	97	97	93	63	56	29	16	9	94	85	29	61
f_{09}	99	-	97	99	96	88	38	21	12	91	96	57	72
f_{11}	99	96	-	99	62	63	29	16	12	100	94	41	65
f_{12}	96	99	100	-	93	91	40	22	13	99	100	69	75
f_{13}	74	93	69	84	-	100	71	37	16	62	87	97	72
f_{14}	66	88	74	93	100	-	76	34	19	71	93	100	74
f_{15}	22	34	24	35	71	66	-	82	46	28	44	99	50
f_{16}	12	21	13	18	28	26	74	-	85	18	22	47	33
f_{17}	6	7	9	13	15	18	40	81	-	13	16	24	22
f_{20}	93	88	100	96	63	68	32	19	13	-	96	43	65
f_{21}	87	94	100	100	93	99	51	22	15	99	-	84	77
f_{22}	41	65	43	62	96	100	100	56	29	46	71	-	64
Average	63	71	66	72	71	70	53	37	24	65	73	63	61





Results Using GPS

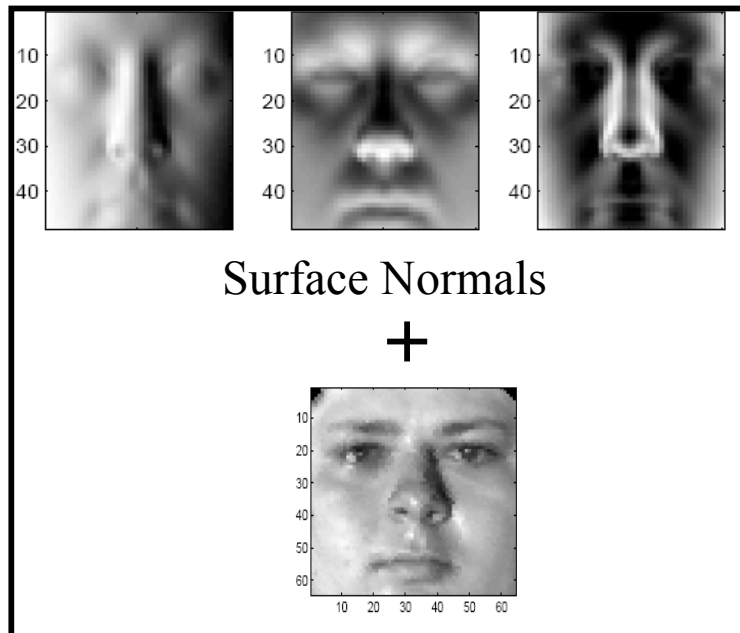


Gallery	f_{08}	f_{09}	f_{11}	f_{12}	f_{13}	f_{14}	f_{15}	f_{16}	f_{17}	f_{20}	f_{21}	f_{22}	Average
Probe													
f_{08}	100	100	100	100	97	91	79	62	40	100	96	84	87
f_{09}	100	100	100	100	100	100	96	87	69	100	99	99	96
f_{11}	100	100	100	100	99	99	93	71	49	100	100	96	92
f_{12}	100	100	100	100	100	100	100	91	81	100	100	100	98
f_{13}	100	100	100	100	100	100	100	100	94	100	100	100	100
f_{14}	97	100	100	100	100	100	100	99	99	100	100	100	100
f_{15}	82	96	87	100	100	100	100	100	100	91	100	100	96
f_{16}	66	79	75	91	100	00	100	100	100	75	97	100	90
f_{17}	56	69	68	84	93	97	100	100	100	71	90	99	86
f_{20}	99	100	100	100	99	100	94	74	60	100	100	99	94
f_{21}	99	100	100	100	100	100	100	97	87	100	100	100	99
f_{22}	94	99	99	100	100	100	100	100	100	100	100	100	99
Average	91	95	94	98	99	99	97	90	82	95	99	98	95





Image Formation Model



Surface Normals

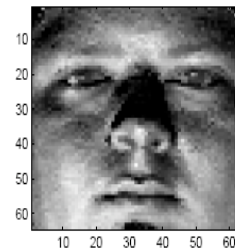
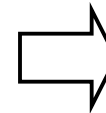
+



Albedo

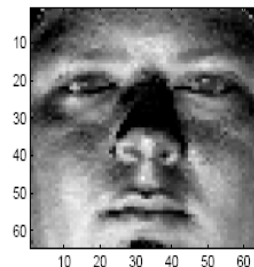
+

Light Source

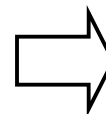


Intensity Image

Inverse Problem



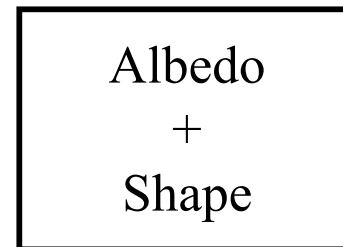
Single Intensity Image



Albedo

+

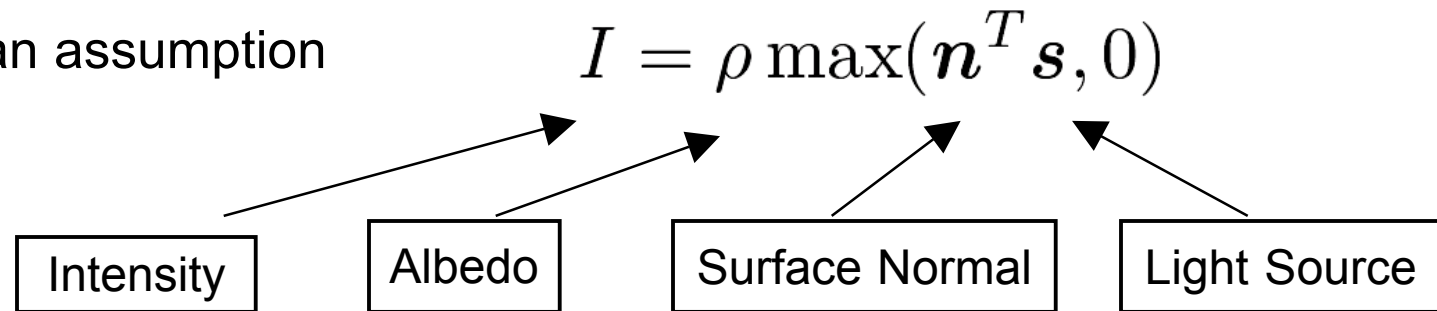
Shape





Albedo Estimation

- Lambertian assumption

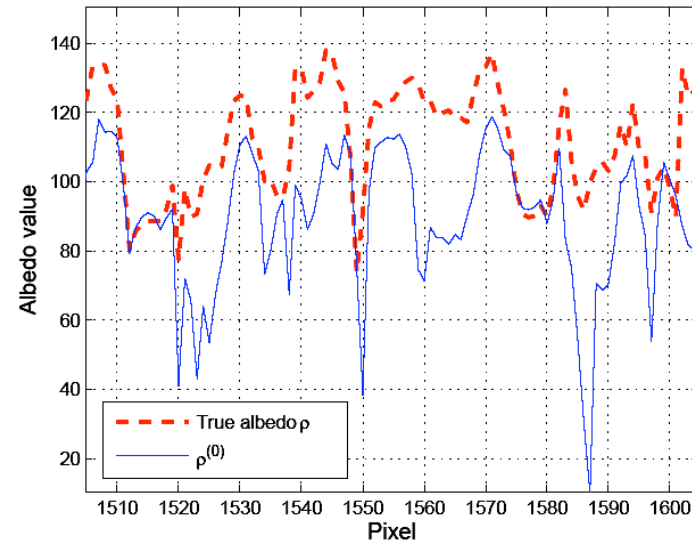


- Light Source Estimated : $\mathbf{s}^{(0)}$

- Initial Surface Normal : $\mathbf{n}_{i,j}^{(0)}$

$$\rho_{i,j}^{(0)} = \frac{I_{i,j}}{\mathbf{n}_{i,j}^{(0)} \cdot \mathbf{s}^{(0)}}$$

Initial Albedo Estimate



Error in initial albedo estimate

Image Estimation Framework

Initial Albedo Estimate $\rho_{i,j}^{(0)} = \frac{I_{i,j}}{\mathbf{n}_{i,j}^{(0)} \cdot \mathbf{s}^{(0)}} = \rho_{i,j} \frac{\mathbf{n}_{i,j} \cdot \mathbf{s}}{\mathbf{n}_{i,j}^{(0)} \cdot \mathbf{s}^{(0)}}$

$$\rho_{i,j}^{(0)} = \rho_{i,j} + \frac{\mathbf{n}_{i,j} \cdot \mathbf{s} - \mathbf{n}_{i,j}^{(0)} \cdot \mathbf{s}^{(0)}}{\mathbf{n}_{i,j}^{(0)} \cdot \mathbf{s}^{(0)}} \rho_{i,j} \quad \Rightarrow \quad \rho_{i,j}^{(0)} = \rho_{i,j} + \mathbf{w}_{i,j}$$

Signal Dependent
Additive Noise

- ❑ Non-stationary Mean Non-stationary Variance (NMNV) model for true albedo
- ❑ Unbiased source assumption and Uncorrelated Noise
- ❑ Biswas, Agarwal and Chellappa, ICCV 2007.

LMMSE Estimate: NMNV MODEL

$$\hat{\rho}_{i,j} = (1 - \alpha_{i,j})E(\rho_{i,j}) + \alpha_{i,j}\rho_{i,j}^{(0)}$$

Ensemble Average
Of Albedo

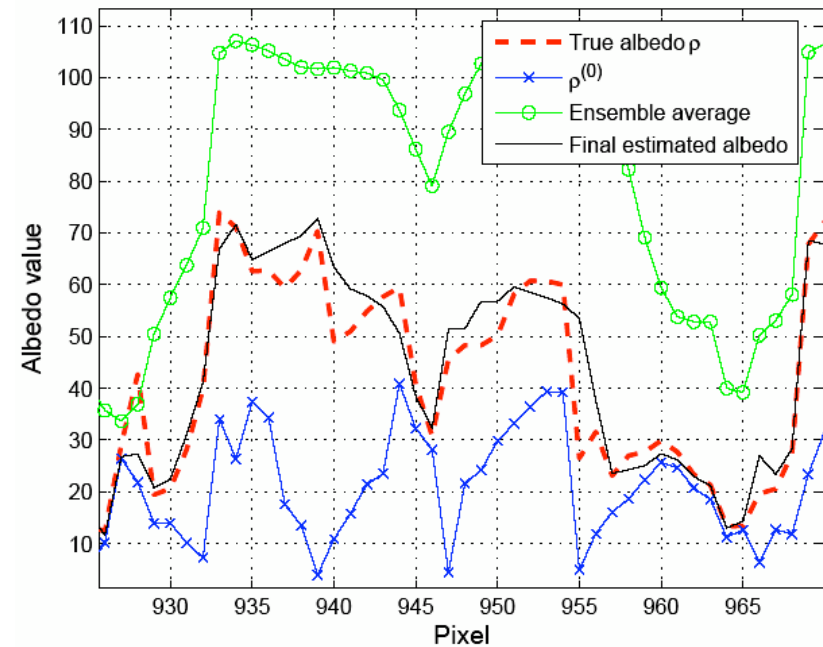
Approximate
Albedo Estimate

where,

$$\alpha_{i,j} = \frac{\sigma_{i,j}^2(\rho)}{\sigma_{i,j}^2(\rho) + \sigma_{i,j}^2(w)}$$

Signal
Variance

Noise
Variance



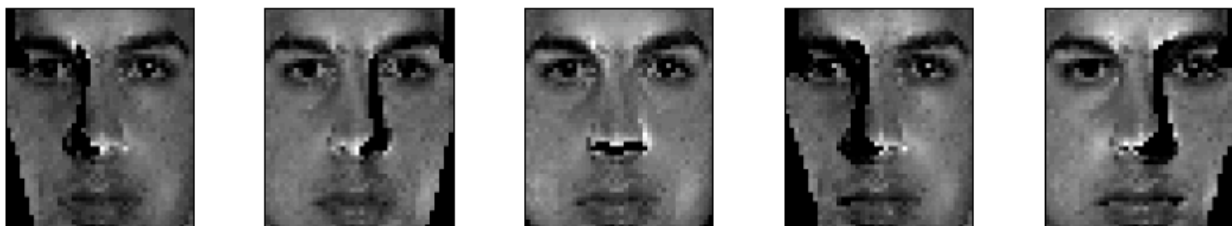


Estimated Albedo – PIE Dataset

Input Image



Noisy Albedo



Estimated Albedo





Relighting Using the Estimated Albedo





Albedo-based Face Recognition

Probe	f_{08}	f_{09}	f_{11}	f_{12}	f_{13}	f_{14}	f_{15}	f_{16}	f_{17}	f_{20}	f_{21}	f_{22}	Avg	Avg [14]	Avg [31]
Gallery															
f_{08}	-	100	100	99	93	91	79	72	44	100	96	85	87	89	92
f_{09}	100	-	100	100	99	97	91	90	75	100	99	93	95	93	97
f_{11}	100	100	-	100	100	97	88	78	57	100	100	93	92	92	95
f_{12}	99	99	100	-	100	100	96	96	87	100	100	97	98	96	98
f_{13}	99	99	100	100	-	100	99	99	90	99	100	100	99	98	100
f_{14}	97	99	100	100	100	-	99	97	90	100	100	100	98	99	99
f_{15}	84	94	88	100	100	100	-	100	99	93	100	100	96	96	97
f_{16}	76	97	79	99	100	99	99	-	100	75	99	100	93	91	94
f_{17}	53	82	56	90	96	94	94	100	-	54	96	97	83	80	87
f_{20}	100	100	100	100	100	100	94	78	57	-	100	99	93	91	95
f_{21}	99	99	100	100	100	100	93	94	85	100	-	97	97	96	99
f_{22}	90	99	97	100	100	100	100	97	91	97	100	-	97	98	98
Avg	91	97	93	99	99	98	94	91	80	93	99	96	94	-	-
Avg [14]	88	94	93	97	99	99	96	89	75	93	98	98	-	93	-
Avg [31]	90	97	94	99	99	99	98	93	87	95	99	99	-	-	96



Shape-based Face Recognition

Probe	f_{08}	f_{09}	f_{11}	f_{12}	f_{13}	f_{14}	f_{15}	f_{16}	f_{17}	f_{20}	f_{21}	f_{22}	Avg
Gallery													
f_{08}	-	99	99	94	88	74	53	47	26	97	85	57	74
f_{09}	94	-	94	99	99	94	71	66	46	93	99	79	85
f_{11}	99	99	-	100	99	96	74	57	46	100	100	87	87
f_{12}	91	99	100	-	100	100	96	87	71	100	100	99	95
f_{13}	87	93	97	100	-	100	99	94	90	96	99	100	96
f_{14}	71	96	97	100	100	-	100	99	94	100	100	100	96
f_{15}	60	76	75	96	100	100	-	100	100	82	97	100	90
f_{16}	41	69	54	90	96	100	100	-	100	62	93	100	82
f_{17}	28	44	47	84	93	97	100	100	-	59	88	99	76
f_{20}	94	96	100	100	97	96	85	60	57	-	100	91	89
f_{21}	85	99	100	100	100	100	97	93	79	100	-	99	96
f_{22}	59	84	85	99	100	100	100	100	100	96	99	-	93
Avg	74	87	86	97	97	96	89	82	74	90	96	92	88

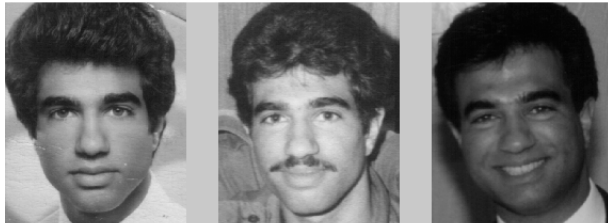


Novel View Synthesis



Facial Similarity across Aging/disguises

Age Progression



4 years

5 years

10 years

1 year

Pose Variations



Illumination and Disguise



How do the above factors affect facial similarity ?

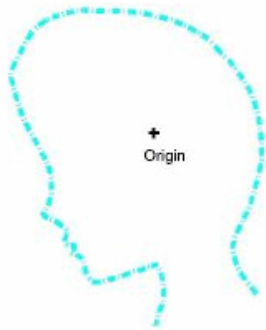


Modeling Age Progression in Young Faces

- Challenges :
 - Facial growth depends on factors such as gender, ethnicity, age group etc.
 - Facial features grow at different rates during different ages : During infancy and during adolescence, growth spurts are observed over different facial features.
- Previous work :
 - Researchers from psychophysics, studied craniofacial growth as a result of internal forces acting on the human cranium.
 - Cardioidal strain, spiral strain, affine shear etc. are some of the transformations that were applied on infant faces (profile views) to study age transformation effects.

Craniofacial Growth models

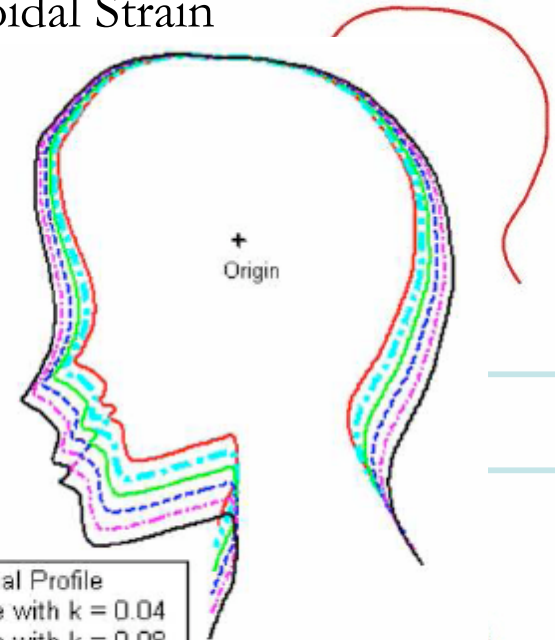
Affine Shear



$$y_1 = y_0$$

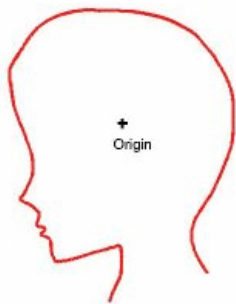
$$x_1 = x_0 + ky_0$$

Cardioidal Strain



- Original Profile
- - - Profile with $k = 0.04$
- Profile with $k = 0.08$
- - - Profile with $k = 0.12$
- - - Profile with $k = 0.16$
- Profile with $k = 0.20$

Revised Cardioidal Strain



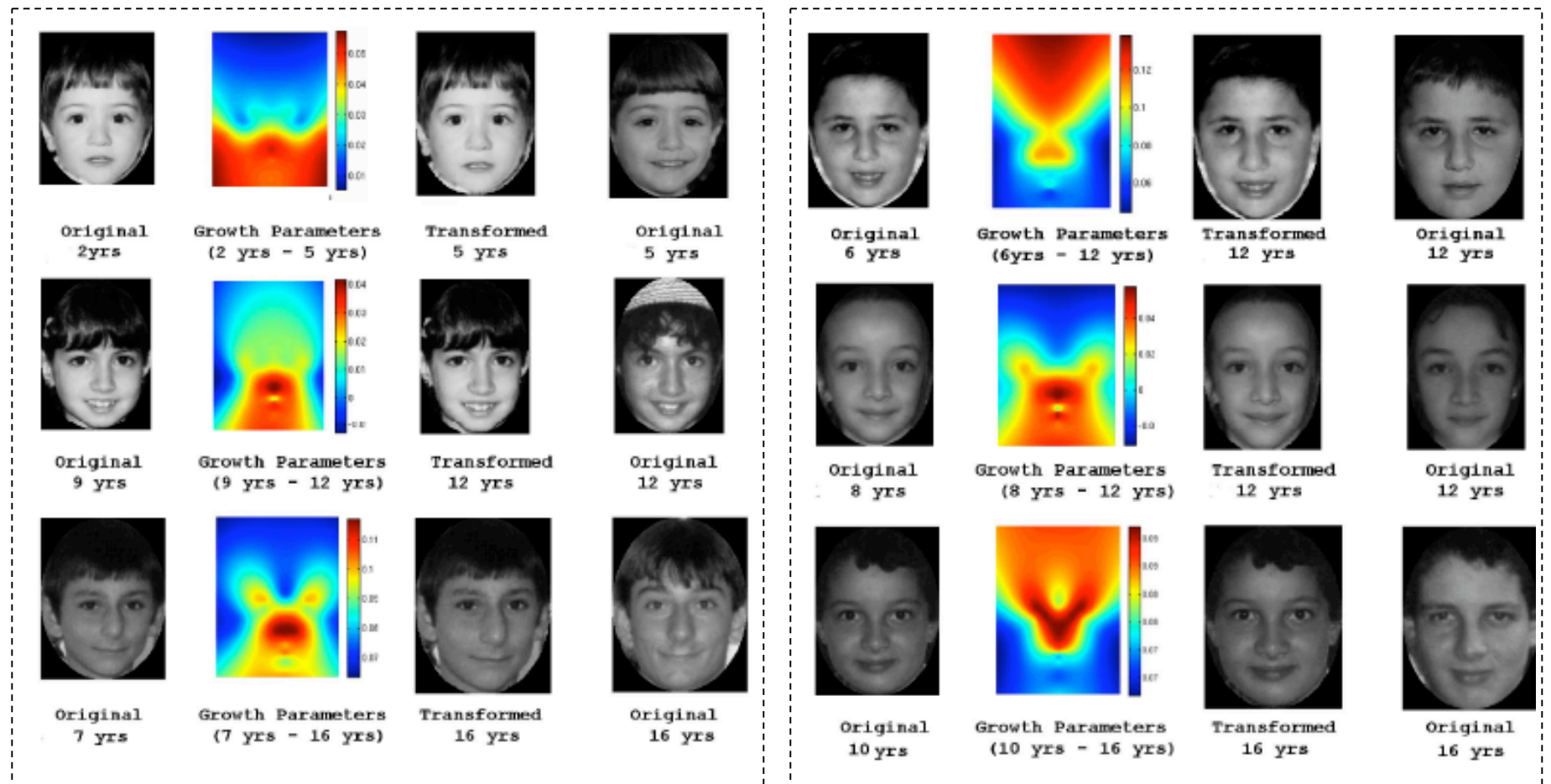
$$R_1 = R_0 + k(R_0 - R_0 \cos(\theta_0))$$

$$\theta_1 = \theta_0$$

Transformations induced by the revised cardioidal strain model reflected growth related transformations best.



Aging Results



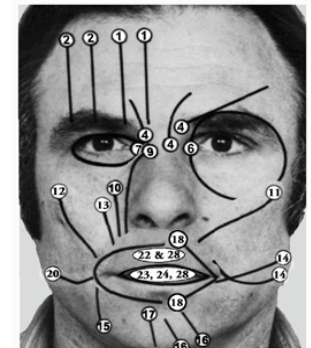
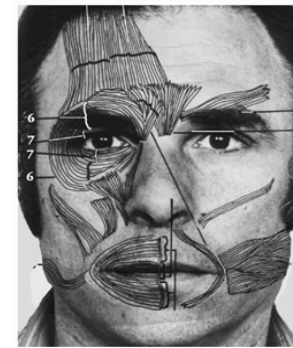
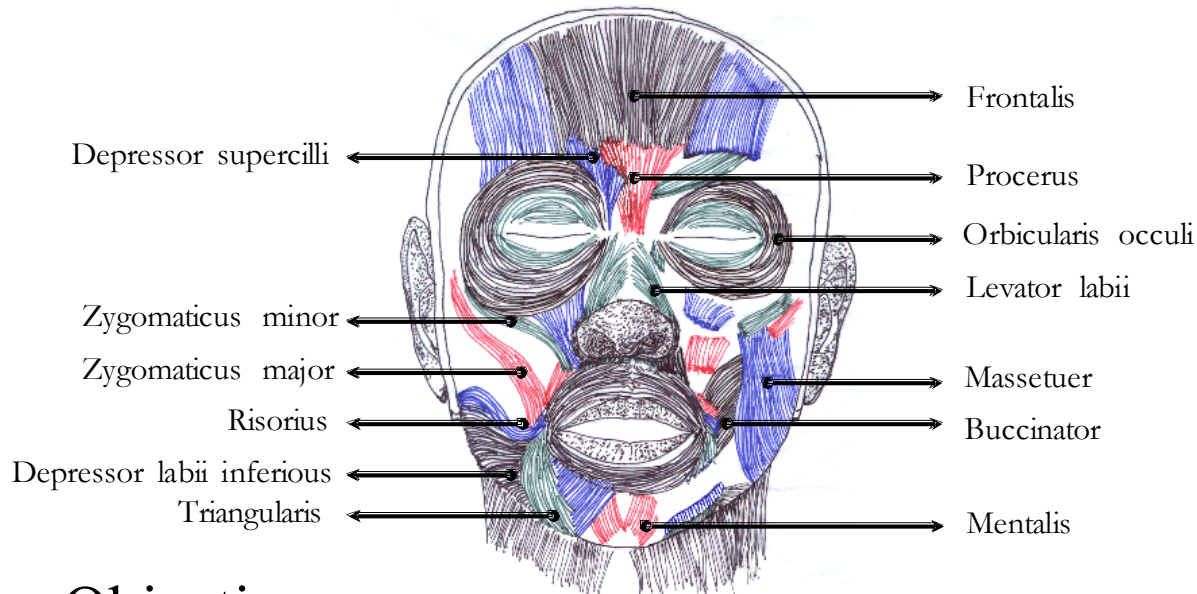


Face Recognition Across Aging

- On a database of 233 images of 109 individuals (a few individuals with multiple age separated images), we perform a face recognition experiments (eigenfaces)
- For each probe image (age known apriori), the gallery images are transformed before performing face recognition.

Approach	Rank 1	Rank 5	Rank 10
No transformation	8	28	44
Age transformed	15	37	58

Modeling Age Progression in Adults

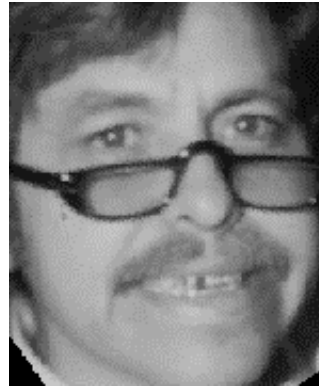
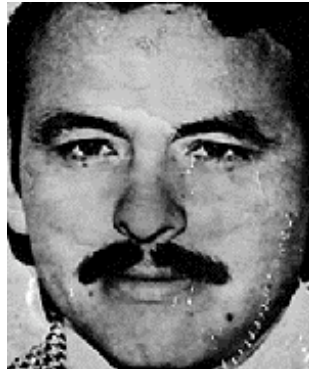


Objectives :

- Characterize elastic properties of facial muscles as a function of age.
- Develop a realistic skin model where wrinkles and other artifacts can be simulated by varying functions of facial muscles.



Disguises





Summary

- Discussed methods for improving the quality of images degraded by pose, illumination variations and aging.
- The effectiveness of image quality improvements should be measured by the resulting increase in recognition rate.